

Using a Mediating Effect in the Electroreduction of Aryldiazonium Salts To Prepare Conducting Organic Films of High Thickness

Marcel Ceccato, Antoine Bousquet, Mogens Hinge, Steen Uttrup Pedersen,* and Kim Daasbjerg*

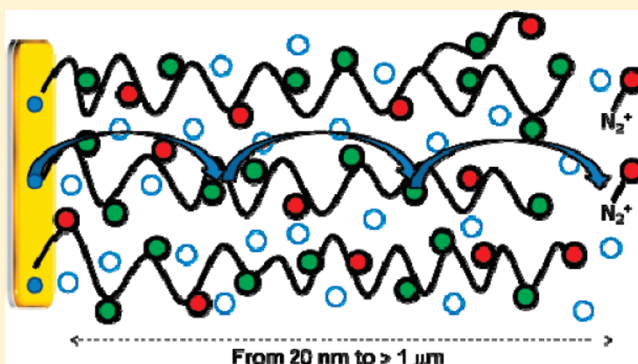
Department of Chemistry, Aarhus University, Langelandsgade 140, DK-8000 Aarhus C, Denmark

Interdisciplinary Nanoscience Center (iNANO), Aarhus University, Ny Munkegade 120, DK-8000 Aarhus C, Denmark

 Supporting Information

ABSTRACT: Usually, electrografting of aryldiazonium salts results in the formation of covalently attached films <10 nm thick. In this work, we report on an electrografting procedure by which thick conducting films, even in the micrometer size range, can be formed on glassy carbon, gold, or stainless steel in a controlled manner. It is a prerequisite that the aryldiazonium salt contains a redox active moiety such as nitrobenzene, anthraquinone, or benzophenone to maintain charge propagation in the growing layer. In addition, electrografting proceeds only efficiently by way of using potential sweeping rather than electrolysis at a fixed potential. Sweeping is essential to continuously desorbing any physisorbed species that otherwise would clog the channels in the film and make it insulating. Cyclic voltammetry, polarization modulation infrared reflection absorption spectroscopy, ellipsometry, and profilometry are used to characterize the surfaces and, through this, explain the growth mechanism. Elucidation of the role of the substrate, solvent, and supporting electrolyte is included in the investigation.

KEYWORDS: aryldiazonium salts, electrografting, mediating effect, conductive polymer, polymer coating, organic film



INTRODUCTION

Preparation of organic films on carbon and metal surfaces is an area of intensive research in surface chemistry. Among the various methods available for accomplishing a covalent attachment, electroreduction of aryldiazonium salt has proven to be highly effective.¹ Because highly reactive aryl radicals are involved in the grafting process, the film is usually a disordered multilayer.² This multilayer, seldom exceeding 10 nm thickness, is an insulator, providing the method with one of its most characteristic features, i.e., a self-limiting film growth. This is due to the fact that the resistance increases as the film grows and at the point, where the driving force of the electrochemically driven grafting process is insufficient to reduce the diazonium salt, the process comes to a halt. Depending on the conditions employed, it is possible, in some cases, to obtain a monolayer.³

To enhance the versatility of the diazonium-based method, it would be important to reveal the circumstances under which films of larger thicknesses and higher conductivities might be prepared. Thick organic layers have very important applications, such as protection of surfaces (for example against corrosion), conductive coatings, or chemical sensors. In 2001, Kariuki and McDermott reported that diethylaniline, phenylacetic acid, and nitrophenyl films 15–25 nm thick could be obtained from the corresponding diazonium salts, using electrolysis for 30 min at an overpotential of 150–300 mV.⁴ In another case reported by

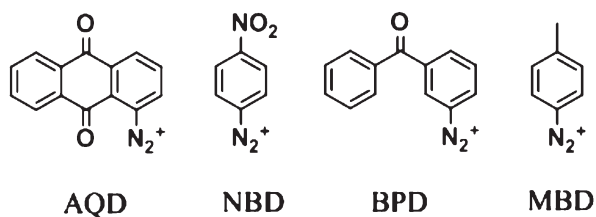
Adenier et al., micrometer-thick conducting polyphenylene film was formed on metals such as Cu and Zn (but not on carbon), employing benzenediazonium salt as a grafting agent.⁵ However, it was noted that any substituent on the benzene ring impeded film formation, which presumably can be attributed to a disruption of the ordered π -system. In a few cases, the redox activity of the immobilized electrochemically active group has been exploited in the film formation. Patents from Bureau et al. describe how thick organic layers of 100 nm thickness could be obtained from the reduction of 4-nitrobenzenediazonium salt by scanning the potential to extreme cathodic potentials (from 0.3 V to -2.9 V vs SCE) for 20 voltammetric cycles.⁶ Haccoun et al. grafted the same salt using repeated cyclic voltammetric sweeps and different switching potentials.⁷ Based on electrochemical quartz crystal microbalance experiments, they reported a steady increase in the mass of the organic layer grafted on a Au substrate. Josselme et al. assembled a few to hundreds of layers of ruthenium *tris*-bipyridine complexes via the diazonium route, using both sweeping and potentiostatic electrodeposition.⁸ Recently, Noel and co-workers electrodeposited a naphthoquinone moiety on Au electrodes.⁹ Using the mediating effect of the latter in the reduction of the corresponding diazonium salt, they could

Received: November 19, 2010

Revised: January 25, 2011

Published: February 15, 2011

Scheme 1. Diazonium Salts Employed in This Study



control the thicknesses to be 1–4 layers by adjusting the potential and the deposition time.

In this work, we use potential sweeping on aryl diazonium salts to form conducting films with thicknesses, even in the micrometer range, on various substrates in a controlled manner. Although the method itself already has been described in the literature, no systematic study has been carried out so far pertaining to the effect of the substrate, solvent, and supporting electrolyte, as well as experimental parameters such as sweep rate and switching potential. Moreover, a profound feature of the diazonium salts selected herein is that they contain an electrochemically active functionality, which provides the assembled film with the redox units required for maintaining charge propagation during the grafting process. We will show that the redox potential of this unit, along with its chemical stability, are determining factors for its efficiency as a mediator and, hence, the film growth. At the same time, the use of potential sweeping is found to be essential for continuously desorbing any physisorbed species that otherwise would clot the channels in the film and make it insulating.

Three diazonium salts, 9,10-dioxo-9,10-dihydroanthracene-2-diazonium (AQD), 4-nitrobenzenediazonium (NBD), and 4-benzoylbenzenediazonium (BPD), have been chosen, because of their electrochemically active substituent (Scheme 1) having different redox properties (*vide infra*). Moreover, 4-methylbenzenediazonium (MBD) salt with the electroinactive tolyl group was included in the study for comparative reasons. Note that, in contrast to the ruthenium complexes previously investigated,⁸ the reduced forms of these redox systems are much more reactive as bases, and, hence, they may be involved in side reactions that will have pronounced indirect effects on the film growth.

RESULTS AND DISCUSSION

Previously, these aryl diazonium salts have been used to functionalize surfaces with anthraquinone,¹⁰ nitrophenyl,¹¹ or benzophenone moieties.¹² However, the redox activity of the functional groups was not exploited during the grafting in any of these cases. Instead, the applied grafting potential was fixed at a potential located between the reduction potentials of the diazonium salt and the redox active group. Under these conditions, the thickness of the film ranged from 1.5 nm to 10.5 nm.^{11a}

Figure 1 shows successive cyclic voltammograms of NBD recorded at a gold plate in 0.1 M Bu₄NBF₄/CH₃CN in the potential range from 0.5 to −1.6 V vs SCE. We may note the appearance of a reduction wave of the diazonium moiety at $E_{p1} = 0.3$ V vs SCE, followed by a second reduction wave at $E_{p2} = -1.4$ V vs SCE, which is attributed to the reduction of the nitrophenyl group to its radical anion. On the reverse sweep, the wave pertaining to the oxidation of the nitrophenyl radical anion is evident.

In addition to these general voltammetric features, two unusual behaviors are seen. First, the reduction wave of the diazonium salt is almost unaltered after 10 cycles which stands in sharp contrast to

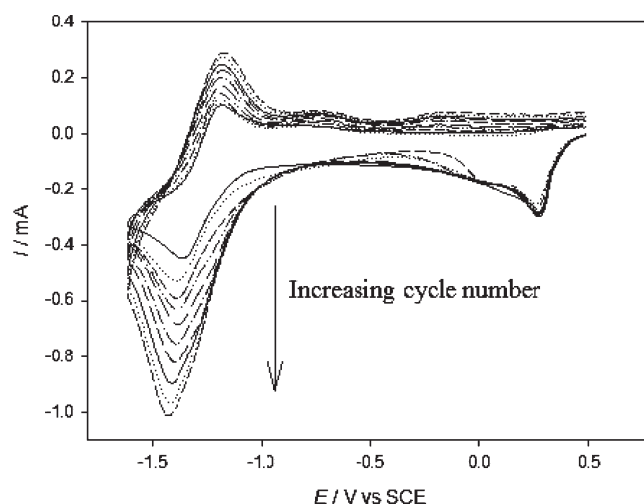


Figure 1. Successive voltammograms recorded in 0.1 M Bu₄NBF₄/CH₃CN containing 2 mM NBD, using a sweep rate of 1 V s^{−1} at a gold plate.

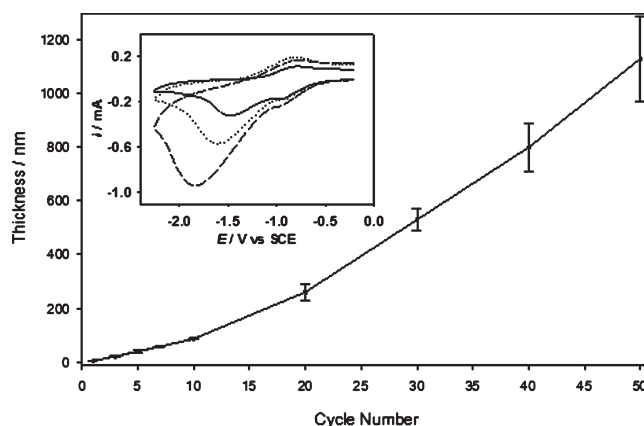


Figure 2. Plot of film thickness as a function of cycle number, where the sweeping is performed in a solution of 2 mM NBD in 0.1 M Bu₄NBF₄/CH₃CN, using a sweep rate of 1 V s^{−1} at a gold electrode. Inset shows the first cyclic voltammogram recorded at a sweep rate of 2 V s^{−1} in 0.1 M Bu₄NBF₄/CH₃CN at a gold electrode that has been modified with NBD using (—) 3, (···) 5, and (---) 10 cyclic voltammetric sweeps.

the blocking of the surface usually seen in the electrografting of diazonium salts. Second, a concomitant increase is observed in the intensity of the redox waves of the nitrophenyl moiety, which would point to a steady increase in the number of redox groups attached to the surface. This development is confirmed by the recording of infrared spectra of the surfaces by means of polarization modulation infrared reflection absorption spectroscopy (PM-IRRAS). As the modification proceeds, a distinct increase occurs in the 1530 and 1350 cm^{−1} bands, corresponding to the asymmetric and symmetric stretching of O–N=O in the nitro group, respectively; stretching of the benzene ring appears as a band at 1600 cm^{−1} (see Figure S1 in the Supporting Information).

The continuous film growth is further evidenced by measuring film thickness (by ellipsometry or profilometry) as a function of cycle number, as shown in Figure 2. Initially, an almost-linear relationship is obtained with a slope of 8.5 nm per cycle, hence giving a thickness of the assembled film of 85 nm after as few as 10 cycles. Upon an additional 40 cycles, the thickness reaches the

micrometer range with no view of a halt in the effectiveness of the growth mechanism. In fact, the growth even seems to become increasingly faster above a thickness of 100 nm, which presumably can be attributed to a surface roughening of the film (see Figure S2 in the Supporting Information). Note that there is no reason to expect a linear relationship between thickness and cycle number, considering the complexity of the radical-based grafting mechanism, as well as the fact that the layer properties change as the grafting proceeds.

The formation of such thick films for a diazonium salt approach is, in itself, remarkable; however, of equally importance, in this respect, is the observation that the film thickness can be controlled precisely through the number of cycles used. As expected, the electrochemical response from the nitrophenyl groups in the film is strongly dependent on the film thickness and therefore also the cycle number. The inset in Figure 2 shows the increase in the electrochemical signal from films immobilized on gold employing 3, 5, and 10 cycles and having thicknesses of 19.8, 39.2, and 85 nm, respectively.

Similar results were obtained with high reproducibility, if the grafting was carried out on glassy carbon (GC) as the substrate (see Figure S3 in the Supporting Information). This allowed determination of the surface coverages through an integration of the cyclic voltammetric wave. Specifically, 1 and 10 cycles resulted in films having thicknesses of 2.9 and 86.3 nm and corresponding surface coverages of $(8.5 \pm 1.1) \times 10^{-10}$ and $(6.3 \pm 0.2) \times 10^{-9}$ mol cm⁻². Hence, while the thickness ratio between the two films is ~ 30 , the ratio of the coverages is only ~ 7 . That a 1:1 relationship is not seen between the thickness and the signal size can be explained by considering that some nitrophenyl groups in the film will be electroinactive, because they either are inaccessible to the electrolyte or have been irreversibly reduced during the grafting process.¹³ Indeed, once radical anions of nitrophenyl are formed, they may be protonated by the residual water always present in CH₃CN, before reoxidation can take place on the reverse sweep.

In this respect, our systems deviate somewhat from the ruthenium *tris*-bipyridine complexes,⁸ where the amount of deposited complexes through the mediating effect was found to grow linearly with the integrated electrical charge. Hence, the high electrochemical and chemical stability (in the absence of diazonium salts) of the ruthenium complexes ensures that they are not deactivated in the film, but all retain their electrochemical activity, even if hundreds of layers are formed.

To elucidate the effect of the switching potential (E_λ), a series of experiments were carried out, in which E_λ was set at a progressively more negative potential, going from -0.2 V to -1.9 V vs SCE. In each specific case, 10 consecutive cycles were carried out to create films, the thickness of which could be easily measured by ellipsometry or profilometry.

Figure 3 shows the plot of the film thickness as a function of E_λ . The pronounced sigmoidal shape obtained can be split into three regions: (a) for $E_\lambda > -0.8$ V vs SCE, the thickness is ~ 10 nm, in accordance with that reported in the literature^{11a} and, by and large, independent of E_λ ; (b) for $-0.8 > E_\lambda > -1.5$ V vs SCE, a large increase in thickness is observed, until (c) for $E_\lambda < -1.5$ V vs SCE, a new plateau value is reached (~ 85 nm). This figure is an exact reflection of the redox properties of the nitrophenyl group probed by cyclic voltammetry (see Figure 1), in which the wave raises precisely in region (b). This means that by "enhancing" E_λ from -0.8 V to -1.5 V vs SCE, an increasingly larger fraction of the nitrophenyl groups becomes reduced, thereby allowing the thickness of the layer to increase.

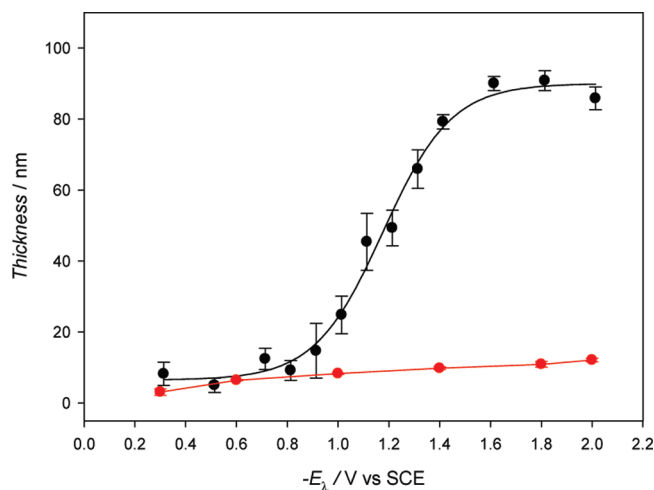
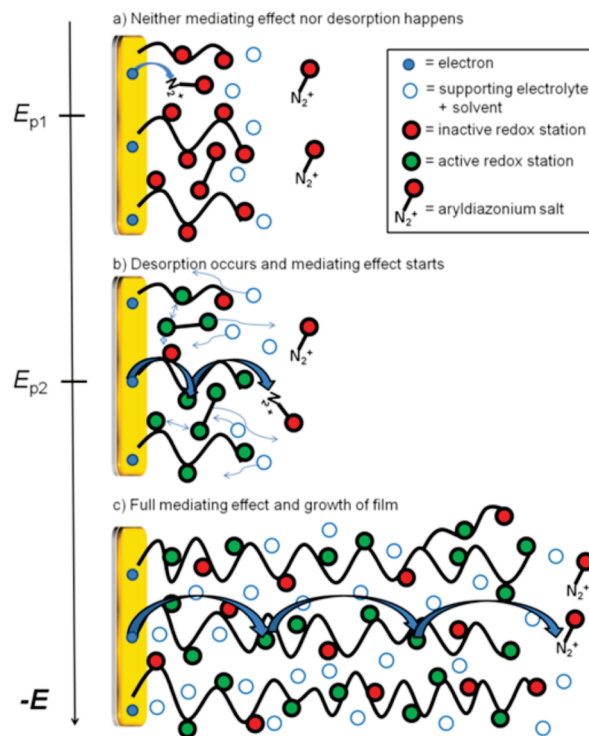


Figure 3. Film thickness on gold surfaces, electrografted from 2 mM solutions of NBD (black line) or MBD (red line) in 0.1 M Bu₄NBF₄/CH₃CN using 10 consecutive cyclic voltammetric cycles at a sweep rate of 1 V s⁻¹ for varying values of E_λ .

Scheme 2. Cartoon Describing the Mechanism of Film Growth during Potential Sweeping



On this basis, we propose that the large increase in thickness happens through a mediating effect, in which electrons from the electrode surface are transported efficiently, via nitrophenyl redox units located throughout the layer, to the diazonium salt adsorbed at the interface (see panel c in Scheme 2). The necessity of having redox groups for sustaining the grafting process is evidenced by carrying out a corresponding set of measurements for MBD, characterized by having the electrochemically inactive tolyl group as a chemical functionality. As seen in Figure 3, the increase in thickness, in this case, is small, reaching only 10 nm at $E_\lambda = -1.8$ V vs SCE.

In addition to serving as redox relay stations, the nitrophenyl groups fulfill another important purpose. Upon charging, they keep the layer structure open by creating channels in the film for the electrolyte/solvent system to access (see panels b and c in Scheme 2). As discussed elsewhere, this happens through a continuous expulsion of the nitrophenyl-containing physisorbed material, which also becomes negatively charged as the potential is swept past E_{p2} .¹³ In this respect, the sweeping itself, which is envisioned to induce a continuous reorganization of the layer structure, turns out to be essential for the desorption process to be efficient. For instance, if the surface film was created rather by way of an electrolysis using an applied potential of -1.5 V vs SCE, the film growth comes to a halt already at a thickness of 4 nm.

In contrast, for ruthenium *tris*-bipyridine complexes,⁸ deposition could be carried out at constant applied potentials, indicating that the adsorption phenomena noted herein pose no or only small problems for the larger organometallic systems. Actually, in these cases, the deposition resembles electropolymerization (both sweeping and controlled potential) of, e.g., vinyl-substituted monomer metal complexes on surfaces, which produces stable and adherent films on surfaces with well-defined electrochemical responses.¹⁴ However, it is noteworthy that, if the mediating effect is not exploited in the grafting process of ruthenium complexes, an insulating layer will be formed just after a few voltammetric sweeps.¹⁵

A further confirmation of the importance of the mediating effect is obtained from an experiment, where the grafting of **NBD** [$E_{\lambda} = -0.6$ V vs SCE, i.e., $E_{\lambda} > E_{p2}$ ($= -1.4$ V vs SCE) to avoid reduction of the nitrophenyl moiety] and the desorption ($E_{\lambda} = -2.2$ V vs SCE, i.e., $E_{\lambda} < E_{p2}$ to ensure that desorption occurs through a reduction of the nitrophenyl moiety) are performed in two different solutions on turns (see Figure S4 in the Supporting Information). In this case, where the mediating effect is precluded, the layer growth reaches only 5 nm. Hence, both the mediating effect and the creation of an open film structure with access for the electrolyte/solvent system are prerequisites for providing the film with a high conductivity throughout the grafting process.

Many other factors could easily be imagined to exert an effect on the film formation. Among these are the nature of the aryldiazonium salt, substrate, solvent, sweep rate, and supporting electrolyte. Hence, we set out to do a survey study on the effect of a change in either of these parameters with the objective of revealing tendencies rather than creating the thickest possible film. Specifically, water (0.1 M KCl/H₂O)¹⁶ and CH₃CN without or with supporting electrolyte (0.1 M Bu₄NBF₄) were selected as solvent systems. In addition to gold, GC and stainless steel (304 S) were considered as substrates. The diazonium salts **BPD** and **AQD** were included, along with **NBD** and **MBD**, to elucidate the role of the functional group.

In Table 1, all results are collected. As observed, the presence of a reducible functional group (as in **AQD**, **NBD**, and **BPD**) is essential to obtain thick films (>20 nm). The anthraquinone, nitrophenyl and benzophenone functionalities, having standard potentials (E^0) of -0.90 , -1.27 , and -1.85 V vs SCE, respectively (measured in cyclic voltammetry at a gold electrode, using a sweep rate of 1 V s⁻¹ in 0.1 M Bu₄NBF₄/CH₃CN; see Figure 1), all possess this capability (entries 1–6 and 9–14 in Table 1). At the same time, this indicates that, to obtain the mediating effect, there are only few restrictions on the choice of the functional group, as long as it is reducible. It is also important to point out that the film growth in these cases could easily be continued, if desired, by simply increasing the number of sweeps.

Table 1. Film Thickness Measured by Ellipsometry for Electrografted Organic Films^a

entry	diazonium salt	substrate ^b	electrolyte/solvent	thickness (nm)
1	AQD	GC	Bu ₄ NBF ₄ /CH ₃ CN	25.0 ± 2.4
2		Au	Bu ₄ NBF ₄ /CH ₃ CN	59.4 ± 0.5
3		Au	KCl/H ₂ O	80.3 ± 5.8
4	NBD	304 S	Bu ₄ NBF ₄ /CH ₃ CN	24.5 ± 4.2
5		GC	Bu ₄ NBF ₄ /CH ₃ CN	86.3 ± 1.6
6		Au	Bu ₄ NBF ₄ /CH ₃ CN	85.0 ± 5.6
7		Au	CH ₃ CN	15.8 ± 1.6
8		Au	KCl/H ₂ O	9.8 ± 1.0
9 ^c	BPD	Au	Bu ₄ NBF ₄ /CH ₃ CN	406 ± 66
10 ^d		Au	Bu ₄ NBF ₄ /CH ₃ CN	891 ± 100
11		304 S	Bu ₄ NBF ₄ /CH ₃ CN	47.8 ± 3.1
12		GC	Bu ₄ NBF ₄ /CH ₃ CN	28.4 ± 2.0
13		Au	Bu ₄ NBF ₄ /CH ₃ CN	36.0 ± 4.7
14		304 S	Bu ₄ NBF ₄ /CH ₃ CN	58.2 ± 7.7
15		304 S	CH ₃ CN	9.1 ± 1.4
16	MBD	304 S	KCl/H ₂ O	5.8 ± 1.3
17		Au	Bu ₄ NBF ₄ /CH ₃ CN	9.7 ± 2.0

^a Grafting performed in a 2 mM solution of the respective diazonium salt by 10 cyclic voltammetric cycles, using a sweep rate of 1 V s⁻¹, unless otherwise noted. Switching potential, E_{λ} , was set at a potential 200–500 mV negative of the reductive peak potential of the mediator (all relevant cyclic voltammograms are collected in Figures S5–S21 in the Supporting Information). ^b Legend: GC, glassy carbon; Au, gold; and 304 S, stainless steel. ^c Performed by means of 20 voltammetric cycles using a sweep rate of 2 V s⁻¹. ^d Performed by means of 100 voltammetric cycles using a sweep rate of 10 V s⁻¹.

In contrast, without the presence of an electrochemically reducible functional group, only thin films can be created. This is the case for **MBD**, where neither desorption nor a mediated electron transport can take place. As a result, the film thickness does not exceed 10 nm in this case, independent of the potential used (see entry 17 in Table 1 and Figure 2).

A closer examination of the results indicates that the nitrophenyl group is more efficient than the anthraquinone and benzophenone moieties in sustaining the growth (compare entries 5, 6, and 11 with entries 1, 2, 4, and 12–14 in Table 1). This is due to the fact that the radical anions of the surface immobilized nitrophenyl moiety possess a sufficiently high reducing capacity ($E^0 = -1.27$ V vs SCE; vide supra) to reduce the **NBD** salt ($E_{p1} = 0.3$ V vs SCE; vide supra) with a high rate while, at the same time, having the required kinetic stability against being irreversibly protonated by the residual water in CH₃CN; this would otherwise form an electroinactive moiety upon further reduction. Hence, under the conditions outlined in Table 1, a high conductivity of the layers can be retained throughout the grafting period and film with thicknesses larger than 80 nm are the result (see entries 5 and 6 in Table 1).

The basicity of the radical anions becomes, in particular, an important issue with the **BPD** salt. With the much more negative reduction potential of the benzophenone moiety ($E^0 = -1.85$ V vs SCE; vide supra), the radical anions are not only extremely potent reducing agents but also are strong bases that are protonated comparatively faster.¹⁷ The result is that the pertinent films become 30–50 nm thinner (entries 12–14). In this respect, the radical anions of anthraquinone with their much lower basicity and, hence, slower deactivation (being, in this

sense, much more comparable to the ruthenium complexes previously studied)^{8,15} should show their supremacy; nevertheless, however, films of the same size as produced for the BPD salt are formed (entries 1, 2, and 4 in Table 1). The most likely explanation for this is the decrease in the driving force (E^0 of the anthraquinone moiety = -0.9 V vs SCE; vide supra) for the reduction of AQD, which would induce a relatively slower reduction rate and thus film growth.

The importance of these issues becomes even clearer, if they are combined with the effect of changing the solvent from CH_3CN to a protic medium such as water. The immediate consequence of this is that films <10 nm thick are formed for BPD (entry 16 in Table 1) and NBD (entry 8 in Table 1). In accordance with expectations, PM-IRRAS analysis could confirm that the carbonyl group of the benzophenone moiety has been irreversibly reduced and deactivated during sweeping (see Figure S21 in the Supporting Information). Interestingly, in the case of AQD a film as thick as 80.3 nm is obtainable, presumably because of the especially low basicity of the radical anions of anthraquinone (entry 3 in Table 1). Indeed, for this redox system only, reversibility is maintained in cyclic voltammetry in water.

To construct thicker films, the application of higher sweep rates is advantageous (compare entries 6, 9, and 10 in Table 1). In these three entries, we have kept the grafting time constant (i.e., the number of sweeps was increased by a factor of 10 if the sweep rate was set 10 times higher). It may be noted that an enhancement of the sweep rate by a factor of 10 and 100 leads to film thicknesses of as much as 400 and 900 nm, respectively. The main explanation for this is presumably that layer opening, in terms of the adsorption/desorption process, will take place more often as the number of sweeps increases within a given time frame. Notably, this potential-induced reorganization of the layers creates a porous film structure being more easily penetrable by the electrolyte/solvent system. Accordingly, not only does the film growth rate increase, but the electrochemical response of the pertinent films also becomes comparatively larger.

Concerning the substrate effect, thick films can be obtained for all three substrates: e.g., a film of 58.2 nm is obtained for BPD on stainless steel (entry 14 in Table 1), a film of 59.4 nm is obtained for AQD on Au (entry 2 in Table 1), and a film of 86.3 nm is observed for NBD on GC (entry 5 in Table 1). However, some apparent variations are also seen that could point to effects from the underlying substrate. In the case of AQD the film thickness of 59.4 nm on Au is more than twice that obtained on GC (25.0 nm; see entry 1 in Table 1) and stainless steel (24.5 nm; see entry 4 in Table 1). For NBD, the layer is thinner on stainless steel (47.8 nm; see entry 11 in Table 1) than on GC (86.3 nm; see entry 5 in Table 1) and Au (85.0 nm; see entry 6 in Table 1). In contrast, for BPD, the layer is thickest on stainless steel (58.2 nm; see entry 14 in Table 1), compared to that on GC (28.4 nm; see entry 12 in Table 1) and Au (36.0 nm; see entry 13 in Table 1). The most likely explanation of this is that the final film structure is very sensitive to the exact structure of the initial layers formed at the surface, which again is affected by the nature of the substrate. Still, at this point, we are not able to give good explanations for the rather diverse variations observed for the three salts combined.

Experiments carried out without the supporting electrolyte, Bu_4NBF_4 (entries 7 and 15 in Table 1), show that its presence is essential for having a successful film growth. The supporting electrolyte takes care of ion transport in the film, with the tetrabutylammonium ion serving the indispensable role as the counterion for the redox moiety upon reduction. Therefore, we

can assume that the electron transfer is mediated by the electroactive substituent only when the layer becomes accessible to the supporting electrolyte. The “diffusion-controlled” appearances of the cyclic voltammograms in the inset of Figure 2 can be explained by this effect, possibly in combination with the effect from electron transfer (or electron hopping) between the electroactive groups, requiring self-diffusion of the polymer chains to achieve the appropriate orientation of these groups.

CONCLUSION

Cyclic voltammetric sweeping on aryldiazonium salt carrying an electroactive moiety allows the formation of thick conducting films, even in the micrometer size range, in a controlled manner. The method can successfully be carried out on various types of conducting materials such as carbon and metals. In many aspects, the electrochemical behavior resembles that of electroactive polymers but with the important notion that the films produced herein are covalently attached at the surfaces. The growth mechanism involves two concomitant phenomena, i.e., continuous layer opening through desorption of physisorbed species and the mediating effect. In this respect, the use of the sweeping technique is essential for the diazonium salts studied herein, noticing that the film growth comes to a halt already at a thickness of a few nanometers, if the surface film is created by way of electrolysis.

The redox moieties are the central units in the transport of electrons from the surface to aryldiazonium molecules at the outer layer. In particular, surface-immobilized nitrophenyl groups are found to be efficient, because of the fact that they, upon reduction, are able to reduce the corresponding diazonium salt with a high rate while, at the same time, having the required chemical stability against being irreversibly protonated by the residual water in CH_3CN . Importantly, the effect from the latter process can easily be overcome by increasing the sweep rate (or eventually use a more carefully dried solvent) to enhance the film growth greatly. In future studies, it would be interesting to investigate the prospect of using these thick films, which exhibit large electrochemical signals, as sensors.

EXPERIMENTAL SECTION

Materials. Acetonitrile (anhydrous, 99.9%, Lab-Scan) was dried prior to electrochemical experiments by passing it through a column of activated (i.e., heated to 350°C under vacuum) Al_2O_3 (99.99%; Sigma–Aldrich). After this treatment, the water content was determined to be 0.03 ± 0.01 wt % by Karl Fisher titration (TitraLab 980; Radiometer Analytical). Water was triple distilled. Tetrabutylammonium tetrafluoroborate (Bu_4NBF_4) was synthesized using standard procedure. 9,10-Dioxo-9,10-dihydroanthracene-2-diazonium (AQD), 4-nitrobenzenediazonium (NBD), 4-benzoyl-benzenediazonium (BPD), and 4-methylbenzenediazonium (MBD) tetrafluoroborates were synthesized from the corresponding anilines, according to standard procedures.¹⁸ Further purification consisted of recrystallization from acetonitrile and diethyl ether, filtration, vacuum drying, and storage at -18°C . Anilines and ferrocene (Sigma–Aldrich) were used without further purification.

Substrates. Glassy carbon (GC) plates (Sigradur G, HTW, $10\text{ mm} \times 10\text{ mm} \times 1\text{ mm}$) were cleaned by sonication in acetone and hexane (1 h in each solvent). Gold plates (glass plates coated with 20 nm of Ti and 200 nm of Au, using physical vapor deposition, $10\text{ mm} \times 10\text{ mm} \times 1\text{ mm}$, Polyteknik, Denmark) were immersed in a piranha solution at room temperature for 5 min. Subsequently, the plates were rinsed several times in triple distilled water, followed by acetone and ethanol (10 min each

solvent). Finally, the plates were dried under argon. Stainless steel plates (304 S, electropolished, 10 mm \times 10 mm \times 1 mm) were cleaned via ultrasonication in acetone and ethanol (10 min in each solvent).

Cyclic Voltammetry. A standard three-electrode electrochemical setup (CH Instruments 660B or 601C) consisting of a GC, gold, or 304 S plate as the working electrode, a platinum wire as the auxiliary electrode, and either a Ag/AgI, Ag/AgCl or SCE as the reference electrode, was used in the electrochemical experiments. At the end of each experiment performed in CH₃CN, the standard potential of the ferrocenium/ferrocene couple ($E_{\text{Fc}^+}^0$) was measured, and all potentials were referenced against SCE using a previous determination of $E_{\text{Fc}^+}^0 = 0.41$ V versus SCE in CH₃CN.¹⁹

An important experimental condition for all measurements is that the electrodes were not immersed in the solution until just before the experiment was started. This minimizes the occurrence of spontaneous adsorption of the aryldiazonium salt at the electrode. Moreover, in the case of already prepared films, the effect of using various soaking times could be left out of consideration.

Electrografting was performed by cyclic voltammetry, using repetitive cycles going to a predetermined switching potential E_{λ} at a sweep rate of 1 V s⁻¹. The grafting solution consisted of 2 mM aryldiazonium salt in dry 0.1 M Bu₄NBF₄/CH₃CN or 0.1 M KCl/water (both degassed using argon). After the electrografting was finished, the plates were ultrasonicated for 10 min in acetone and dried under a stream of argon.

Ellipsometry. Thicknesses of films (in the dry state; the films are dried under an argon flow after ultrasonication) were measured using a rotating analyzer ellipsometer (Dre, Germany). The GC plates were measured at a 65° angle of incidence, while gold and 304 S were measured at 75°. The ellipsometric parameters of the bare (Δ_0 , ψ_0) and grafted (Δ_g , ψ_g) substrates were measured in air at ambient temperature, where Δ is the phase shift and $\tan \psi$ is the amplitude ratio upon reflection. The complex refractive index of the bare substrate was calculated from the measured Δ_0 and ψ_0 values. A three-layer optical model, consisting of a substrate with a complex refractive index, the grafted layer with a refractive index n_f and thickness d_f , and the surrounding medium (air) was used to calculate the overall reflection coefficients for in-plane (R_p) and out-of-plane (R_s) polarized lights.

The real and imaginary parts of the refractive index of the bare substrate were obtained by measuring the clean plates prior to modification. Ellipsometric measurements were performed on the same area of the plates before and after electrografting. Because the measurements are carried out on dried (and, therefore, collapsed) films, the refractive index of the layer is fixed at a constant value (real = 1.55; imaginary = 0), independent of the thickness. The average values and the standard deviations reported correspond to data points obtained from measuring three spots on each plate.

Profilometry. Thickness profiles for films were measured using Dektak 150 Surface Profiler from Veeco Instrument, Inc. The thickness was determined on the dry film from a cross-sectional profile across the film using the substrate edges as reference for the bare substrate. Alternatively, a scratch made using a plastic tip was employed as a reference.

Polarization Modulation Infrared Reflection Absorption Spectroscopy (PM-IRRAS). Polarization modulation infrared reflection absorption spectroscopy (PM-IRRAS) spectra were recorded on a Bio-Rad FTS 65A (Randolph, MA) FTIR-spectrometer that was equipped with an external PM-IRRAS module with a narrow bandwidth mercury–cadmium–telluride (MCT) detector cooled in liquid nitrogen. The infrared beam was modulated at 74 kHz between s- or p-polarization by combining a gold wire polarizer with Hinds ZnSe photoelastic modulator (PEM-90/II/ZS37). The PEM device was adjusted so that the s-polarization was linear for wavenumbers at 1500 cm⁻¹. The gold and stainless steel substrates were irradiated with an incident grazing angle of 80°. The two signals, $R_p - R_s$, and $R_p + R_s$, were extracted with a high-pass filter (EG&G model 189), adjusted to

40 kHz, and a lock-in amplifier (SR 810 DSP) and digitized sequentially as 20 spectra of each signal in 20 cycles (in total 800 spectra). The differential surface reflectivity spectra were obtained with a 4 cm⁻¹ resolution. The experimental PM-IRRAS spectra were normalized with respect to a bare substrate and finally baseline-corrected using cubic splines in the Digital Resolution Pro 4.0 program. All spectra were recorded at room temperature in a dry atmosphere.

■ ASSOCIATED CONTENT

S Supporting Information. Cyclic voltammograms pertaining to Table 1, PMIRRAS spectra, and profilometry data. This material is available free of charge via the Internet at <http://pubs.acs.org>.

■ AUTHOR INFORMATION

Corresponding Author

*E-mail addresses: sup@chem.au.dk (S.U.P.), kdaa@chem.au.dk (K.D.).

■ ACKNOWLEDGMENT

The Danish Agency for Science, Technology and Innovation, Grundfos and SP Group are gratefully acknowledged for financial support.

■ REFERENCES

- (1) (a) Barrière, F.; Downard, A. J. *J. Solid State Electr.* **2008**, *12*, 1231–1244. (b) Onclin, S.; Ravoo, B. J.; Reinhoudt, D. N. *Angew. Chem., Int. Ed.* **2005**, *44*, 6282–6304. (c) Love, J. C.; Estroff, L. A.; Kriebel, J. K.; Nuzzo, R. G.; Whitesides, G. M. *Chem. Rev.* **2005**, *105*, 1103–1169. (d) Pinson, J.; Podvorica, F. *Chem. Soc. Rev.* **2005**, *34*, 429–439.
- (2) (a) Combellas, C.; Kanoufi, F.; Pinson, J.; Podvorica, F. I. *Langmuir* **2005**, *21*, 280–286. (b) Kariuki, J. K.; McDermott, M. T. *Langmuir* **1999**, *15*, 6534–6540.
- (3) (a) Malmos, K.; Iruthayaraj, J.; Pedersen, S. U.; Daasbjerg, K. *J. Am. Chem. Soc.* **2009**, *131*, 13926–13927. (b) Malmos, K.; Dong, M.; Pillai, S.; Kingshott, P.; Besenbacher, F.; Pedersen, S. U.; Daasbjerg, K. *J. Am. Chem. Soc.* **2009**, *131*, 4928–4936. (c) Combellas, C.; Kanoufi, F.; Pinson, J.; Podvorica, F. I. *J. Am. Chem. Soc.* **2008**, *130*, 8576–8577. (d) Nielsen, L. T.; Vase, K. H.; Dong, M.; Besenbacher, F.; Pedersen, S. U.; Daasbjerg, K. *J. Am. Chem. Soc.* **2007**, *129*, 1888–1889. (e) Stewart, M. P.; Maya, F.; Kosynkin, D. V.; Dirk, S. M.; Stapleton, J. J.; McGuinness, C. L.; Allara, D. L.; Tour, J. M. *J. Am. Chem. Soc.* **2004**, *126*, 370–378. (f) Leroux, Y. R.; Fei, H.; Noël, J.-M.; Roux, C.; Hapiot, P. *J. Am. Chem. Soc.* **2010**, *132*, 14039–14041.
- (4) Kariuki, J. K.; McDermott, M. T. *Langmuir* **2001**, *17*, 5947–5951.
- (5) Adenier, A.; Combellas, C.; Kanoufi, F.; Pinson, J.; Podvorica, F. I. *Chem. Mater.* **2006**, *18*, 2021–2029.
- (6) (a) Bureau, C.; Levy, E.; Viel, P. U.S. Patent 2004/0248428 A1, 2004. (b) Bureau, C.; Levy, E.; Viel, P. PCT Int. Appl. WO 03018212, 2003.
- (7) Haccoun, J.; Vautrin-UI, C.; Chaussé, A.; Adenier, A. *Prog. Org. Coat.* **2008**, *63*, 18–24.
- (8) Jousseme, B.; Bidan, G.; Billon, M.; Goyer, C.; Kervella, Y.; Guillerez, S.; Hamad, E. A.; Goze-Bac, C.; Mevellec, J.-Y.; Lefrant, S. *J. Electroanal. Chem.* **2008**, *621*, 277–285.
- (9) March, G.; Reisberg, S.; Piro, B.; Pham, M.-C.; Fave, C.; Noël, V. *Anal. Chem.* **2010**, *82*, 3523–3530.
- (10) Kullapere, M.; Tammeveski, K. *Electrochem. Commun.* **2007**, *9*, 1196–1201.
- (11) (a) Laforgue, A.; Addou, T.; Bélanger, D. *Langmuir* **2005**, *21*, 6855–6865. (b) Hinge, M.; Ceccato, M.; Kingshott, P.; Besenbacher, F.; Pedersen, S. U.; Daasbjerg, K. *New J. Chem.* **2009**, *33*, 2405–2408.

- (12) Adenier, A.; Cabet-Deliry, E.; Lalot, T.; Pinson, J.; Podvorica, F. *Chem. Mater.* **2002**, *14*, 4576–4585.
- (13) (a) Brooksby, P. A.; Downard, A. *Langmuir* **2004**, *20*, 5038–5045. (b) Ceccato, M.; Nielsen, L. T.; Iruthayaraj, J.; Hinge, M.; Pedersen, S. U.; Daasbjerg, K. *Langmuir* **2010**, *26*, 10812–10821.
- (14) Denisevich, P.; Abrura, H. D.; Leidner, C. R.; Meyer, J.; Murray, R. W. *Inorg. Chem.* **1982**, *6*, 2153–2161.
- (15) Agnès, C.; Arnault, J.-C.; Omnès, F.; Jousselme, B.; Billon, M.; Bidan, G.; Mailley, P. *Phys. Chem. Chem. Phys.* **2009**, *11*, 11647–11654.
- (16) Combellas, C.; Delamar, M.; Kanoufi, F.; Pinson, J.; Podvorica, F. I. *Chem. Mater.* **2005**, *17*, 3968–3975.
- (17) Lund, H.; Hammerich, O. *Organic Electrochemistry*, 4th ed.; Marcel Dekker: New York, 2001; pp 411–434.
- (18) Klamann, D. *Methoden der Organischen Chemie*, 4th ed.; Padeken, H.-G., Ed.; Georg Thieme Verlag: Stuttgart, Germany, 1990; Vol. 2, Chapter 5, p 1060.
- (19) Daasbjerg, K.; Pedersen, S. U.; Lund, H. In *General Aspects of the Chemistry of Radicals*; Alfassi, Z. B., Ed.; Wiley: Chichester, U.K., 1999; pp 385–427.